Low Overhead MIMO-OTFS Channel Estimation

Kailong Wang
Dept. of Electrical and Computer Engineering
Rutgers University, Piscataway, NJ 08854, USA

Athina Petropulu
Dept. of Electrical and Computer Engineering
Rutgers University, Piscataway, NJ 08854, USA

***Abstract*—The paper considers channel estimation for orthogonal time frequency space (OTFS) systems operating in high-frequency, high-mobility scenarios. Existing OTFS channel estimation approaches embed pilots within the OTFS burst in the Delay-Doppler (DD) domain, surrounded by large guard regions to prevent interference from neighboring DD domain symbols during channel propagation. This results in significant bandwidth overhead. In MIMO systems, the DD domain pilots and their guard regions must be non-overlapping across antennas, which constrains scalability. In this paper, we propose a novel channel estimation approach for MIMO OTFS systems that requires significantly less overhead as compared to existing methods. Our approach embeds pilots in the TF domain of certain antennas with guard bins in the TF and DD domains. The TF guard bins ensure that a pilot bin is used exclusively by its respective antenna, while the DD guard bins ensure that the enforcement of TF domain pilots and guard bins does not result in loss of DD domain information. Based on the symbols received on the pilot bins, the receiver can estimate the channel parameters by formulating and solving a sparse signal recovery problem based on the discretization of the target space. The problem complexity can be significantly reduced if the receiver has coarse estimates of the channel parameters, which help constrain the search space. Such estimates may be derived from past observations or provided by a transmitter equipped with integrated sensing and communication (ISAC) capabilities. The proposed approach dramatically reduces pilot overhead as compared to state-of-the-art existing methods (0.006% versus 7% for the same channel and system setup), and enables seamless scalability to large MIMO systems.**

***Index Terms*—OTFS, channel estimation, embedded pilots**

I. Introduction

Multiple-input multiple-output (MIMO) [1] and orthogonal frequency division multiplexing (OFDM) [2] are key technologies for meeting the demands of modern wireless communication systems, ensuring both reliability and efficiency. OFDM has gained popularity due to its ability to support high communication rates and its robustness to frequency-selective fading. MIMO-OFDM systems have been successfully adopted in 5G standards [3]. However, OFDM performance degrades in high-frequency, high-mobility scenarios—key use cases targeted by 6G systems [4]. The recently proposed Orthogonal Time Frequency Space (OTFS) waveform [5] effectively handles such environments by employing a Doppler-delay (DD) channel representation. In the DD domain, the time-varying channels caused by high-frequency, high-mobility environments are sparsely represented and appear linear time-invariant, enabling accurate equalization and signal detection.

The work was supported by ARO grant W911NF2320103 and NSF grant ECCS-2320568.

Accurate channel state information (CSI) at the receiver is critical for achieving high-quality communication. Pilot-aided CSI estimation for single-input single-output (SISO) systems using pilots embedded in the DD domain OTFS burst was proposed in [6], where pilots are safeguarded by zero guard regions. Exploiting the sparse nature of the DD channel, the CSI can be determined by a threshold-based method. This embedded design allows for both channel estimation and symbol detection within a single OTFS burst, leading to a low bit error rate (BER). However, the requirement for guard regions reduces the communication rate by imposing approximately a 30% overhead under a 3GPP standardized channel with 6 dominant paths. For MIMO channel estimation, non-overlapping pilots with dedicated guard regions for different transmit antennas were proposed in [7]. However, this approach does not scale well to large arrays. To support large MIMO systems, overlapped i.i.d. pilots are proposed in [8], [9], where the channel is estimated via Sparse Bayesian Learning (SBL) [8], or Block Sparse Bayesian Learning (BSBL) [9]. While this design reduces the overhead compared to non-overlapping methods, it still requires long pilot sequences, incurring a pilot overhead of approximately 7% [8], [9] under the 3GPP EVA model with 3 dominant paths.

OTFS channel estimation has also been studied using bursts of pilots transmitted between OTFS data frames [10], [11]. While this approach is compatible with large MIMO systems, it can degrade equalization and symbol detection performance due to outdated channel state information. In high-mobility scenarios, an embedded pilot design is preferred, as scatterers may remain in range for only a short duration. Moreover, time-domain pilot bursts result in significant bandwidth waste.

In this paper, we propose a novel embedded pilot design for MIMO OTFS systems that significantly reduces overhead compared to existing approaches. We embed pilots in the TF domain and enforce guard bins in the TF and DD domains. Unlike existing approaches [6], [7], where the guard bins ensure that DD domain pilots will not overlap with other symbols after passing through the channel; in our proposed method, the TF guard bins ensure that the TF pilots are private to the corresponding antenna, and the DD domain information-bearing symbols are preserved despite enforcing pilots and guard bins in the TF domain. Based on the pilots received on the private bins, assuming a sparse DD-domain channel (*i.e.*, a small number of scatterers in the signal's path), the receiver can formulate and solve a sparse signal recovery (SSR) problem to estimate the angles, Doppler, delays, and reflection coefficients

of the scatterers in the signal path. With this newly acquired CSI, equalization can then be performed. The SSR complexity can be significantly reduced if the receiver has coarse estimates of the channel parameters, which help constrain the search space. Such estimates may be derived from past observations or provided by a transmitter equipped with integrated sensing and communication (ISAC) capabilities. While our proposed guard bins and pilots represent overhead, only a small number of them is sufficient to achieve high-quality channel estimates with minimal communication rate loss. For the total number of N_p pilots in the TF domain, $N_p(N_t-1)$ guard bins are needed in the TF domain and N_tN_p guard bins are needed in the DD domain. The overall overhead is $N_tN_p/(N_tNM)$, which is much smaller than that of using guard regions in the literature. The proposed system is robust to Doppler frequency shifts encountered in high-mobility scenarios, is easily scaled to large MIMO systems, and enables in-burst CSI acquisition with minimal bandwidth overhead.

II. MIMO-OTFS Channel Model

We consider a wireless system comprising a transmitter with N_t transmit antennas, transmitting OTFS waveforms to a communication receiver with N_c antennas. The carrier frequency is f_c Hz, and the wavelength is $\lambda = c/f_c$ with c being the speed of light. The transmit and receive antennas form uniform linear arrays with spacing g_t and g_c, respectively. The modulated binary source data are divided into N_t parallel streams, one for each transmit antenna.

The antennas simultaneously transmit packet bursts, each of a duration $T = N\Delta t$ with bandwidth $B = M\Delta f$; here N is the number of subsymbols, M is the number of subcarriers, Δt is the subsymbol duration, and Δf is the subcarrier spacing. The orthogonality condition requires that $\Delta t \cdot \Delta f = 1$. In each burst, a set of NM symbols are arranged on the DD grid,

$$\{\, [k\Delta\nu, l\Delta\tau] \mid k = 0, 1, \ldots, N-1; l = 0, 1, \ldots, M-1 \,\},$$

where k and l are Doppler and delay indices, and the grid spacing is $\Delta\nu = 1/(N\Delta t),\ \Delta\tau = 1/(M\Delta f)$.

We employ the angular DD domain channel model [11], consisting of J reflectors at angle of arrival (AoA) θ_j and angle of departure (AoD) φ_j, *i.e.*,

$$\boldsymbol{h}(\theta,\varphi,\nu,\tau) = \sum_{j=0}^{J-1} \beta_j \boldsymbol{a}_c(\theta_j)\boldsymbol{a}_t^{\mathsf{H}}(\varphi_j)\delta(\nu-\nu_j)\delta(\tau-\tau_j),$$

where β_j is the channel attenuation factor, $\boldsymbol{a}_c(\theta_j)$ is the AOA steering vector, $\boldsymbol{a}_t(\varphi_j)$ is the AoD steering vector, $\nu_j = 2v_j/\lambda$ is the Doppler of velocity v_j and $\tau_j = R_j/c$ is the delay of range R_j for the j-th reflector, respectively. Each reflector's Doppler and delay can be characterized by the Doppler and delay indices $\nu_j = (k_j + \kappa_j)\Delta\nu$, $\tau_j = l_j\Delta\tau$, where $\kappa_j \in [-1/2, 1/2]$ denotes the fractional Doppler. The impact of fractional delays in typical wideband systems can be neglected [12] since the delay spacing $\Delta\tau$ is sufficiently small. The dimensions of the grid satisfy $N \geq 2\max|k_j| + 1$ and $M \geq \max l_j$, so that it can support all Doppler and delays that are present in the target scene. For high frequency signals, the DD channel is sparse, i.e., $J \ll NM$.

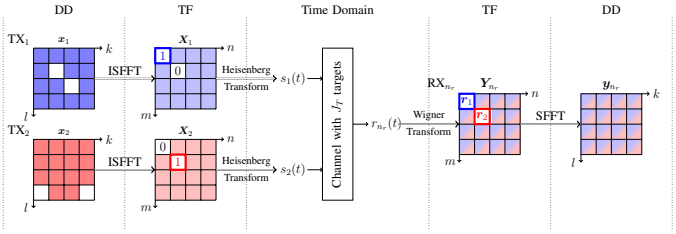

Fig. 1: Pilot bin and guard bins in the TF and DD domains

Let $x_{n_t}[k,l]$ be the symbol of the n_t-th antenna placed on DD bin $[k,l]$. The symbols are mapped to the TF domain via the Inverse Symplectic Finite Fourier Transform (ISFFT) [5].The analog signal for transmission, $s_{n_t}(t)$, is created via the Heisenberg Transform [5].

The noiseless received signal at the n_c-th receive antenna is

$$r_{n_c}(t) = \sum_{j=0}^{J-1} e^{-j2\pi n_c g_c \frac{\sin(\theta_j)}{\lambda}} \sum_{n_t=0}^{N_t-1} e^{-j2\pi n_t g_t \frac{\sin(\varphi_j)}{\lambda}} \times \beta_j s_{n_t}(t-\tau_j) e^{j2\pi\nu_j(t-\tau_j)}. \quad (1)$$

The n_c-th receiver applies a matched filter $g_{cx}(t)$ and samples $r_{n_c}(t)$ over a duration T at frequency B (in other words, it takes the Wigner Transform [5] of $r_{n_c}(t)$). On assuming that the transmitter pulses $g_{tx}(t)$ and $g_{cx}(t)$ are bi-orthogonal, the TF domain channel input-output (I/O) relation corresponding to TF bin $[n,m]$ is

$$Y_{n_c}[n,m] = \sum_{j=0}^{J-1} e^{-j2\pi n_c g_c \frac{\sin(\theta_j)}{\lambda}} \sum_{n_t=0}^{N_t-1} e^{-j2\pi n_t g_t \frac{\sin(\varphi_j)}{\lambda}} \times X_{n_t}[n,m]H^j[n,m], \quad (2)$$

where

$$H^j[n,m] = \beta_j e^{-j2\pi\nu_j\tau_j} e^{j2\pi(\nu_j n\Delta t - m\Delta f\tau_j)}. \quad (3)$$

In matrix form, Eq. (2) becomes $\boldsymbol{Y}_{\text{MIMO}}[n,m] = \boldsymbol{H}_{\text{MIMO}}[n,m]\boldsymbol{X}_{\text{MIMO}}[n,m]$, where $\boldsymbol{Y}_{\text{MIMO}}[n,m] \in \mathbb{C}^{N_c\times 1}$ contains the received TF symbols across all receive antennas; $\boldsymbol{X}_{\text{MIMO}}[n,m] \in \mathbb{C}^{N_t\times 1}$ contains the transmitted TF symbols across all transmit antennas; and $\boldsymbol{H}_{\text{MIMO}}[n,m] \in \mathbb{C}^{N_c\times N_t}$ represents the TF channel between all receive-transmit antenna pairs, with (n_c,n_t)-th element equal to $\sum_{j=0}^{J-1} e^{-j2\pi n_c g_c \frac{\sin(\theta_j)}{\lambda}} e^{-j2\pi n_t g_t \frac{\sin(\varphi_j)}{\lambda}} H^j[n,m]$. Knowing the channel, the TF symbols can be obtained via LMMSE equalization and then brought to the DD domain via an SFFT [5].

III. Embedded Pilots and Guard Bins

The pilots are placed in TF domain bins, which are designated as private to a certain antenna, meaning that those bins are for use by that antenna only. Let the location of pilots on antenna n_t be described by the set $\mathcal{P}_{n_t}$, and $|\mathcal{P}_{n_t}|$ be the size of the set. The total number of pilots is $N_p = \sum_{n_t=0}^{N_t} |\mathcal{P}_{n_t}|$. A private bin $[n_p, m_p]$ for transmit antenna p is created by enforcing zeros in bins $[n_p, m_p]$ of all other transmit antennas. Thus, at the receiver, only the symbol from the p-th antenna is present in bin $[n_p, m_p]$. So, the TF domain zeros can be viewed as guard bins, preserving the private usage of bin $[n_p, m_p]$ by transmit antenna p.

Since each TF bin contains a linear combination of all the DD domain symbols, enforcing one zero or pilot in the TF domain reduces by one the available equations that can be used to recover the DD information from the TF one. This can be mitigated by reducing the number of DD symbols to be recovered by one, via the introduction of one empty DD bin. That empty bin can be viewed as a guard bin, preserving the integrity of the DD domain information.

The above ideas are illustrated in Fig. 1 for the case of $N_t = 2$. In Fig. 1, TF bin $[0, 0]$ is private to TX_1, and pilot symbol 1 is placed in that bin (see blue square frame). At the same time, the bin $[0, 0]$ of TX_2 is set to 0 (guard bin). Bin $[1, 1]$ is private to TX_2 and pilot symbol 1 is placed in that bin (see red square frame). At the same time, bin $[1, 1]$ of TX_1 is set to 0 (guard bin). Since 2 TF bins were changed in each antenna, the TF domain now provides 14 linear equations containing the DD domain symbols. By introducing 2 DD empty bins, there are 14 DD domain symbols. Therefore, despite destroying the 2 TF domain bins to place a pilot and a 0, all the DD information is preserved in the remaining TF bins.

The TF private bins are orthogonal at the receive antennas and can be used to formulate an SSR problem as follows. The receiver knows which bins contain pilots. On private bin $[n_p, m_p]$, the n_c-th receive antenna receives (see Eq. (2))

$$Y_{n_c}[n_p, m_p] = \sum_{j=0}^{J-1} e^{-j2\pi n_c g_c \frac{\sin(\theta_j)}{\lambda}} e^{-j2\pi p g_t \frac{\sin(\varphi_j)}{\lambda}} \times X_p[n_p, m_p] H^j[n_p, m_p], \quad (4)$$

where $X_p[n_p, m_p]$ is the known pilot. Based on the ratio $Y_{n_c}[n_p, m_p]/X_p[n_p, m_p]$ corresponding to all pilots of the n_c-th antenna, the receiver forms the vector $\boldsymbol{r}_p \in \mathbb{C}^{N_c \times 1}$, which can be expressed as

$$\boldsymbol{r}_p = \boldsymbol{\Phi}_p(\theta_j, \varphi_j, \nu_j, \tau_j; n_p, m_p)\boldsymbol{\beta}, \quad (5)$$

where $\boldsymbol{\Phi}_p \in \mathbb{C}^{N_c \times J}$ is a matrix whose (n_c, j)-th element equals $e^{-j2\pi n_c g_c \frac{\sin(\theta_j)}{\lambda}} e^{-j2\pi p g_t \frac{\sin(\varphi_j)}{\lambda}} e^{-j2\pi\nu_j\tau_j} e^{j2\pi(\nu_j n_p \Delta t - m_p \Delta f \tau_j)}$, and $\boldsymbol{\beta} = [\beta_0, \beta_1, \ldots, \beta_{J-1}]^{\mathsf{T}}$. By stacking $\{\boldsymbol{r}_p | p = 1, \ldots, N_p\}$ in vector $\boldsymbol{r} \in \mathbb{C}^{N_c N_p \times 1}$, we get

$$\boldsymbol{r} = \boldsymbol{\Phi}\boldsymbol{\beta}. \quad (6)$$

Each column of $\boldsymbol{\Phi} \in \mathbb{C}^{N_c N_p \times J}$ is constructed based on parameters $(\theta_j, \varphi_j, \nu_j, \tau_j)$ of the j-th path. We can form a matrix $\tilde{\boldsymbol{\Phi}}$ by discretizing this 4D space (the target space) with G_θ, G_φ, G_ν, and G_τ grid points $(\tilde{\theta}_j, \tilde{\varphi}_j, \tilde{\nu}_j, \tilde{\tau}_j)$, respectively. The discretization of Doppler will be a fraction of $\Delta\nu$ to capture fractional Doppler. Then Eq. (6) becomes

$$\boldsymbol{r} = \tilde{\boldsymbol{\Phi}}\tilde{\boldsymbol{\beta}}, \quad (7)$$

where $\tilde{\boldsymbol{\Phi}} \in \mathbb{C}^{N_c N_p \times G_\theta G_\varphi G_\nu G_\tau}$ has elements like $\boldsymbol{\Phi}$ with parameters replaced by the discretized points; $\tilde{\boldsymbol{\beta}} \in \mathbb{C}^{G_\theta G_\varphi G_\nu G_\tau \times 1}$ is a sparse vector with only J non-zero entries corresponding to path parameters. We can obtain $\tilde{\boldsymbol{\beta}}$ by solving a SSR problem via orthogonal matching pursuit (OMP) [13].

A. Reduced Complexity Leveraging Coarse Channel Estimates Provide by an ISAC Transmitter

Discretizing the entire space would result in an unmanageably large matrix $\tilde{\boldsymbol{\Phi}}$. The availability of channel parameter coarse estimates allows for a reduction of the target space, and thus of the complexity of the SSR problem. Next, we describe how a transmitter with ISAC capabilities, as envisioned in 6G [4], can provide coarse channel parameter estimates to the receiver. In this case, the communication channel scatterers would act as targets for the ISAC transmitter, allowing estimation of their Doppler shifts and delays [14], [15], [16].

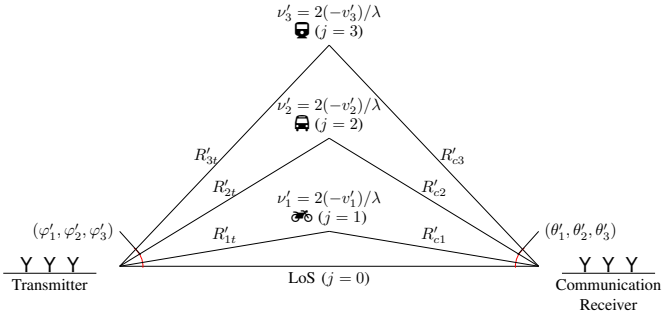

Fig. 2: Bistatic radar geometry model with 3 path scatters.

Assume that the transmitter has previously estimated $(\varphi'_j, v'_j, R'_{jt})$ (see Fig. 2), for example using the method described in [14], [15], [16], and conveyed these values to the communication receiver via the current OTFS burst. In the meantime, the path reflectors may have changed. Assuming that those changes are not large, those estimates can be used by the communication receiver to restrict the target space in the SSR problem.

Suppose the relative speed is directed along the AoD, then φ'_j is the coarse estimates of AoD. The path relative velocity to the communication receiver will have the same magnitude in the opposite direction as that of the transmitter. Then, $\nu'_j = 2(-v'_j)/\lambda$ is the coarse estimates of the path Doppler. Assuming that the distance R_0 between two base stations is generally known and $R'_j = R'_{cj} + R'_{jt}$, we can obtain

$$R'_{cj} = \sqrt{R_0^2 + R_{jt}'^2 - 2R_0 R'_{jt}\cos\varphi'_j}, \quad (8)$$

and

$$\theta'_j = \arccos\frac{R_0^2 + R_{cj}'^2 - R_{jt}'^2}{2R_0 R'_{cj}}, \quad (9)$$

using the law of cosines [17]. Finall, we obtain $\tau'_j = (R'_{cj} + R'_{jt})/c$ as the coarse estimate of the path delay.

The true channel parameters corresponding to the current OTFS burst, *i.e.*, $(\theta_j, \varphi_j, \nu_j, \tau_j)$ will lie in the vicinity of $(\theta'_j, \varphi'_j, \nu'_j, \tau'_j)$. As an example, an OTFS symbol with $\Delta f = 120k\text{Hz}$ and $N = 64$ will have burst time $T = N \times (1/\Delta f) = 0.5222\text{ms}$. A high-speed target in the path with velocity $v = 100\text{m/s}$ will only move 0.05222m per burst. By discretizing the 4D space around the coarse estimates and formulating Eq. (7), the receiver can finetune the true path parameters and estimate β_js, completing channel estimation.

Coarse estimates of the channel parameters could also be available from past channel estimates of the receiver.

B. Communication with Private Bins

The ISFFT can be represented in vector form as $\boldsymbol{X}_p = \boldsymbol{G}\boldsymbol{x}_p$ where $\boldsymbol{X}_p$ has $X_p[n,m]$ in its $(m+nM)$-th position; $\boldsymbol{x}_p$ has $x_p[k,l]$ in its $(l+kM)$-th position; and $\boldsymbol{G} = \mathbf{F}_N{}^{\mathsf{H}} \otimes \mathbf{F}_M$ is the ISFFT matrix with $\mathbf{F}_M$ being the M-points FFT matrix. After considering the guard bins, the TF DD relations of the p-th antenna can be expressed in terms of the modified SFFT, as $\tilde{\boldsymbol{X}}_p = \tilde{\boldsymbol{G}}_p \tilde{\boldsymbol{x}}_p$, where $\tilde{\boldsymbol{X}}_p$ is constructed from $\boldsymbol{X}_p$ by excluding the zero/pilot elements; $\tilde{\boldsymbol{x}}_p$ is constructed from $\boldsymbol{x}_p$ by excluding the empty elements; and $\tilde{\boldsymbol{G}}_p$ is constructed based on $\boldsymbol{G}$, by removing its row corresponding to TF zero/pilot bins and its column corresponding to DD empty bins. We name here $\tilde{\boldsymbol{G}}_p{}^{-1}$ as the modified SFFT. Based on the equalized TF samples, the information-bearing symbols can be obtained by removing the zero/pilot TF bins and then applying the modified SFFT. This assumes knowing the locations of the empty bins in the DD domain and the zero/pilot bins in the TF domain.

C. Overhead Analysis

The proposed method reduces the number of information-bearing symbols by N_t for each TF private bin, resulting in a total pilot overhead of $\eta = N_t N_p/(N_t NM)$. Importantly, our design achieves orthogonality at the receiver, allowing N_p to be significantly smaller compared to existing approaches.

For non-overlapping method [6], [7], the high overhead $\eta = N_t N_p/(N_t NM)$ is due to the large $|\mathcal{P}_{n_t}|$ and N_p. For overlapping i.i.d. DD pilots [8], [9], the overhead is reduced to $\eta = N_t|\mathcal{P}_{n_t}|/(N_t NM)$. For the time domain pilots, the overhead is typically defined as $\eta = N_t|\mathcal{P}_{n_t}|/(N_t NM)$ [10], [11]. The latter two methods need $|\mathcal{P}_{n_t}|$ to be sufficiently large to achieve accurate channel estimation. This is because the underlying algorithm, Sparse Bayesian Learning, relies on a large number of i.i.d. pilots (though they are not orthogonal at the receiver) to construct an accurate posterior distribution.

IV. Simulation Results

In this section, we present simulation results to demonstrate the performance of the proposed system. The path scatterers are simulated on a 2D plane. The transmitter is located at $(0,0)$, and the communication receiver at $(200,0)$, *i.e.*, $R_0 = 200\,\text{m}$. The j-th path scattering point is randomly assigned coordinates $x_j \in [50,150]$ and $y_j \in [-50,50]$, leading to $\varphi_j \in [-45,45]^\circ$ and $R_{jt} \in [50,158]\,\text{m}$. Each scattering point is associated with a relative speed $v_j \in [-100,100]\,\text{m/s}$. We assume a lag of 10 OTFS burst durations, *i.e.*, lag $= 10T$, between the receiver's true channel parameters and the coarse estimates. During that time, the j-th scatter's true coordinates (x_j^*, y_j^*) are updated using $x_j^* = x_j + v_j\cos(\varphi_j)\cdot\text{lag}$ and $y_j^* = y_j + v_j\sin(\varphi_j)\cdot\text{lag}$, assuming the relative velocity v_j remains constant and is directed along the φ_j during this lagged period. The transmitter acquires path estimates $(\varphi_j', v_j', R_{jt}')$ based on [14], [15], [16] and transmits them to the receiver, along with the positions of zero/pilot TF bins and empty DD bins as explained in Section III-A.

The system parameters are detailed in Table I to comply with the 5G NR high-frequency standard [3] for System I and the 5G NR standard [3] for System II. The antenna spacing, denoted as g_t and g_c, is set to 0.5λ, a commonly used configuration.

Table I: System Parameters

Symbol	Parameter	System I	System II
f_c	Carrier frequency	24.25GHz	4GHz
Δf	Subcarrier spacing	120KHz	15KHz
M	Number of subcarriers	2048	512
N	Number of subsymbols	64	128

A. BER Performance of Communication

The bit error rate (BER) evaluated with System I is presented in Fig. 3 for various configurations of SNR, N_t, N_r, and modulation order of QAM, with one pilot per transmit antenna. In each configuration, the channel comprises two scattering paths, as previously described.

The BER when using coarse estimates (dotted line in the figure) is high. However, when those estimates, along with a discretization of the space around them, are used to construct and solve an SSR problem, they result in improved estimates and, thus, an improved BER (solid line). As a benchmark, the BERs, when using the true parameters in equalization, are also shown (dashed line). As expected, higher modulation orders lead to higher BER, and increasing the number of receive antennas results in a reduction in BER.

Additionally, we note that the BER approaches the benchmark more closely at higher modulation orders.

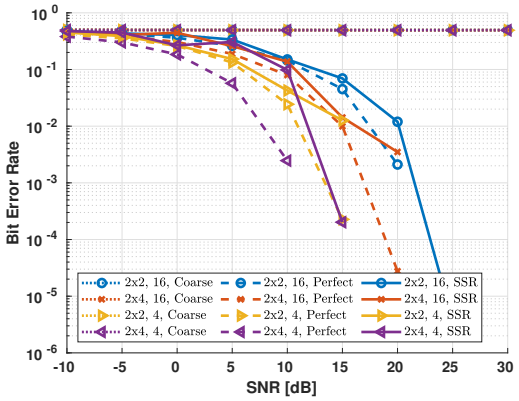

Fig. 3: BER performance comparison.

B. NMSE Performance of Channel Estimation

Here, we evaluate the channel estimation performance of the proposed approach considering a 2×2 MIMO system with 4-QAM modulation and using 200 Monte Carlo trials. In each trial, the target parameters are simulated as described earlier. The performance is evaluated using the normalized mean squared error (NMSE) in [dB] and shown in Fig. 4.

For comparison, we also include the NMSE results of channel estimation via the method of Sparse Bayesian learning (SBL) [8] and Block Sparse Bayesian learning (BSBL) [9], both of which utilize pilot sequences with 7% overhead. The

system parameters, which follow [8], [9], are detailed in the system II of Table I. When SNR ≤ 8 dB, both the SBL and BSBL algorithms exhibit lower NMSE, as the use of pilot sequences effectively mitigates noise with the assistance of additional pilots. When SNR $= 10$ dB, the proposed system outperforms both the SBL and the BSBL algorithms. This improvement is attributed to the orthogonality between TF private bins at the receiver and the compact matrix $\tilde{\mathbf{\Phi}}$, which leverages coarse estimates to reduce coherence and enables SSR to achieve reliable solutions. When SNR $\in [12, 18]$ dB, the SBL algorithm exhibits slower SNR gain and higher NMSE than the proposed system, as it is generalized from SISO systems. While the BSBL algorithm performs better with 1 pilot at SNRs above 12 dB, a small and highly effective adjustment to 2 pilots per antenna allows our proposed method to close this gap and surpass the BSBL algorithm's performance in the $12 \sim 14$ dB SNR range. The pilot overhead of the proposed system is extremely low, *i.e.*, $\frac{N_t N_p}{N_t NM} = \frac{2\times4}{2\times512\times128} \approx 0.006\%$ for $N_t = 2$ and $|\mathcal{P}_{n_t}| = 2$, significantly lower than the 7% overhead of [8], [9] when achieving comparable NMSE under the same setup. Despite the proposed method needing to convey the information of coarse estimates, pilots and guard bins, the overall system overhead will still be lower than the existing methods.

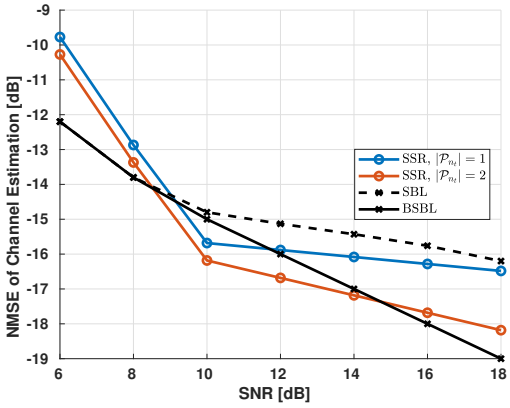

Fig. 4: NMSE performance comparison.

V. Conclusion

We have proposed a novel embedded pilot-aided channel estimation method for MIMO OTFS communication systems. We embed pilots in the TF domain and enforce guard bins in the TF and DD domains. The TF guard bins ensure that different TF domain samples will not overlap after passing through the channel, and the DD guard bins guarantee DD domain information-bearing symbols remain recoverable. The pilot bins from all antennas are used by the receiver to formulate a sparse signal recovery (SSR) problem, whose solution yields high-quality estimates of the scatterers comprising the channel. The SSR performance can be significantly improved by incorporating coarse estimates of the channel scatterers, which may be available during a tracking phase or provided by a transmitter with ISAC capabilities. Simulation results demonstrate that the proposed method achieves comparable NMSE performance with significantly smaller overhead than the existing literature, enabling seamless scalability to large MIMO systems.

References

[1] T. Marzetta, E. Larsson, H. Yang, and H. Ngo, *Fundamentals of Massive MIMO*, ser. Fundamentals of Massive MIMO. Cambridge University Press, 2016. [Online]. Available: https://books.google.com/books?id=IM0iDQAAQBAJ

[2] S. B. Weinstein, "The history of orthogonal frequency-division multiplexing," *IEEE Communications Magazine*, vol. 47, no. 11, pp. 26–35, 2009.

[3] W. Vook, A. Ghosh, E. Diarte, and M. Murphy, "5G New Radio: Overview and Performance," in *2018 52nd Asilomar Conference on Signals, Systems, and Computers*, 2018, pp. 1247–1251.

[4] A. Bourdoux, A. Barreto, B. V. Liempd, C. Lima, D. Dardari, D. Belot, E.-S. Lohan, G. Seco-Granados, H. Sarieddeen, H. Wymeersch, J. Suutala, J. Saloranta, M. Guillaud, M. Isomursu, M. Valkama, M. R. K. Aziz, R. Berkvens, T. Sanguanpuak, T. Svensson, and Y. Miao, "6G White Paper on Localization and Sensing," *arXiv.org*, 2020. [Online]. Available: https://www.semanticscholar.org/paper/6G-White-Paper-on-Localization-and-Sensing-Bourdoux-Barreto/5dff13fddcfdd1d1ff4c2ec93625941d7134d19a

[5] R. Hadani, S. Rakib, M. Tsatsanis, A. Monk, A. J. Goldsmith, A. F. Molisch, and R. Calderbank, "Orthogonal Time Frequency Space Modulation," in *2017 IEEE Wireless Communications and Networking Conference (WCNC)*. San Francisco, CA, USA: IEEE, Mar. 2017, pp. 1–6.

[6] P. Raviteja, K. T. Phan, and Y. Hong, "Embedded Pilot-Aided Channel Estimation for OTFS in Delay–Doppler Channels," *IEEE Transactions on Vehicular Technology*, vol. 68, no. 5, pp. 4906–4917, May 2019.

[7] M. Kollengode Ramachandran and A. Chockalingam, "MIMO-OTFS in High-Doppler Fading Channels: Signal Detection and Channel Estimation," in *2018 IEEE Global Communications Conference (GLOBECOM)*. Abu Dhabi, United Arab Emirates: IEEE, Dec. 2018, pp. 206–212.

[8] L. Zhao, W.-J. Gao, and W. Guo, "Sparse Bayesian Learning of Delay-Doppler Channel for OTFS System," *IEEE Communications Letters*, vol. 24, no. 12, pp. 2766–2769, Dec. 2020.

[9] L. Zhao, J. Yang, Y. Liu, and W. Guo, "Block Sparse Bayesian Learning-Based Channel Estimation for MIMO-OTFS Systems," *IEEE Communications Letters*, vol. 26, no. 4, pp. 892–896, Apr. 2022.

[10] S. Srivastava, R. K. Singh, A. K. Jagannatham, and L. Hanzo, "Bayesian Learning Aided Simultaneous Row and Group Sparse Channel Estimation in Orthogonal Time Frequency Space Modulated MIMO Systems," *IEEE Transactions on Communications*, vol. 70, no. 1, pp. 635–648, Jan. 2022.

[11] ——, "Delay-Doppler and Angular Domain 4D-Sparse CSI Estimation in OTFS Aided MIMO Systems," *IEEE Transactions on Vehicular Technology*, vol. 71, no. 12, pp. 13 447–13 452, Dec. 2022.

[12] D. Tse and P. Viswanath, *Fundamentals of Wireless Communication*, ser. Wiley series in telecommunications. Cambridge University Press, 2005. [Online]. Available: https://books.google.com/books?id=66XBb5tZX6EC

[13] F. Gómez-Cuba and A. J. Goldsmith, "Compressed sensing channel estimation for ofdm with non-gaussian multipath gains," *IEEE Transactions on Wireless Communications*, vol. 19, no. 1, pp. 47–61, 2020.

[14] K. Wang and A. Petropulu, "A Bandwidth Efficient Dual Function Radar Communication System Based on a MIMO Radar Using OTFS Waveforms," accepted by 2025 IEEE International Conference on Acoustics, Speech and Signal Processing (ICASSP).

[15] ——, "Virtual Array for Dual Function MIMO Radar Communication Systems using OTFS Waveforms," 2024, accepted by 5th IEEE International Symposium on Joint Communications & Sensing. [Online]. Available: https://arxiv.org/abs/2411.09777

[16] ——, "Isac mimo systems with otfs waveforms and virtual arrays," 2025. [Online]. Available: https://arxiv.org/abs/2502.01952

[17] M. I. Skolnik, "An analysis of bistatic radar," *IRE Transactions on Aerospace and Navigational Electronics*, vol. ANE-8, no. 1, pp. 19–27, 1961.